PHYSICAL REVIEW D VOLUME 39, NUMBER 1 1 JANUARY 1989

Effect of jet production on the multiplicity dependence of average transverse momentum

Xin-nian Wang and Rudolph C. Hwa
Institute of Theoretical Science and Department of Physics, University of Oregon, Eugene, Oregon 97403
(Received 18 April 1988)

The geometrical branching model for multiparticle production is used to study the multiplicity dependence of the average transverse momentum $\langle p_T \rangle_n$ of charged particles produced in the central region of $p\bar{p}$ collisions. The production of jets is shown to be responsible for the increase of $\langle p_T \rangle_n$ with multiplicity. We demonstrate that beyond the plateau region that follows the initial steep rise the jets cause $\langle p_T \rangle_n$ to have a further increase at even higher multiplicities. The physical basis of this "ledge" effect is discussed and contrasted from an earlier speculation based on phase transition.

I. INTRODUCTION

This is the second in a series of papers on transverse momentum. In Ref. 1 we studied the problem in high-energy nuclear collisions and the formalism used is relativistic hydrodynamics both with and without phase transition. In this paper we consider the problem in high-energy hadronic collisions in the framework of a model on soft interaction with jets. In both papers we examine the multiplicity dependence of the average transverse momentum of produced particles. Since the techniques used are widely different, and the chronology seems to be reversed, some comments on their relationship are in order at the outset.

In Japanese-American Cooperative Emulsion Experiment (JACEE) cosmic-ray experiments[2] the average transverse momentum $\langle p_T \rangle$ is found to increase with the rapidity density of the produced particles until what appears to be a scattered plateau is reached and then to rise again at much higher multiplicities. Theoretically it has been suggested[3] that a flat plateau followed by a sharp rise could signal the formation of quark-gluon plasma. In Ref. 1 we calculated $\langle p_T \rangle$ by taking into consideration the collective transverse expansion, as the system cools through phase transition. It was found that when the initial temperature is varied due to impact-parameter smearing, the observable average transverse momentum tends to a saturated value instead of rising again at high multiplicities. In fact, it is very difficult to obtain a high value for $\langle p_T \rangle$, even if the nuclear size and collision energy are increased. The reason is that the observed particles are produced after the system has cooled down to below the transition temperature, so the value of $\langle p_T \rangle$ is insensitive to the initial temperature of the plasma; moreover, a smearing of the initial temperature from low values (corresponding to large impact parameter) must be carried out. The question then remains: what is the physics that can account for the sharp rise in $\langle p_T \rangle$ observed by JACEE at very high multiplicities?

At that time we conjectured[1,4] that the rise at high multiplicities could have its origin in a new mechanism: namely, jet production. The energies of the relevant cosmic-ray events are certainly high enough to have produced large-p_T jets. Our concern at that time was, however, the effect that color conductivity of the plasma might have on the observable characteristics of the jets, since no color flux tube can develop between two receding partons on the opposite sides of a plasma. While there are numerous complications associated with jet production in high-energy nuclear collisions that must be investigated, it is clear that a beginning should be made at the simplest level, i.e., the study of the effects of jet production on $\langle p_T \rangle$ in hadronic collisions. That is precisely the aim of the paper. The implication on nuclear collisions will be discussed in a subsequent paper.

From low energies up to the CERN ISR energy region ($\sqrt{s} \leq 65$ GeV), a number of features of hadronic collisions are observed to having scaling properties, such as (1) constant $\langle p_T \rangle$, (2) Koba-Nielson-Olesen (KNO) scaling,[5] and (3) constant $\sigma_{\rm el}/\sigma_{\rm tot}$. Feature (3) is usually referred to as geometrical scaling. Feature (2) has recently been related to geometrical scaling in a model[6] in which the Furry branching distribution[7] is smeared over impact parameter. As the energy goes up, all these scaling properties are violated.[8] Furthermore, transverse momentum $\langle p_T \rangle_n$ has been observed to increase with charged multiplicity $n_{\rm ch}$ (Ref. 9 and 10). The phenomenon begins to show up at the top of the ISR energies,[11] but it is at the CERN collider that the trend is fully developed. Since the phenomenon is accompanied by jet production,[12] especially the low-E_T jets (called minijets) observed by the UA1 Collaboration,[10] a simple two-component model[13] has provided an adequate description of $\langle p_T \rangle_n$. More recently, a formalism has been developed[14] for the description of multiplicity distribution at high energies by incorporating the production of low-E_T jets in the geometrical branching model[6] (GBM). It reproduces the violation of KNO scaling quite well[15] and also gives the observed increase of $\sigma_{\rm el}/\sigma_{\rm tot}$ and $\langle n_{\rm ch} \rangle$ with energy. It is our purpose in this paper to show that this formalism also gives the correct dependence of $\langle p_T \rangle_n$ on $n_{\rm ch}$. Because of the two-component structure of the GBM (Ref. 14), $\langle p_T \rangle_n$ will increase with $n_{\rm ch}$ until it reaches a flattened region. At very high multiplicity where the jet contribution to multiplicity is dominant, $\langle p_T \rangle_n$ will rise again until it reaches the average transverse momentum $\langle p_T \rangle_{\rm jet}$ of the particles from jet fragmentation, which is much higher than the $\langle p_T \rangle$ in soft interactions. This

rise-plateau-rise structure in $\langle p_T \rangle_n$ vs n_{ch}, referred to as the "ledge" effect, will be shown to be consistent with the experimental data on $p\bar{p}$ collisions. It is similar in character to the structure seen in the JACEE data, but is drastically different in its origin when compared to the conjecture of Ref. 3.

We briefly review in Sec. II the GBM and refer the readers to Refs. 14 and 15 for details. In Sec. III we derive the dependence of $\langle p_T \rangle_n$ on multiplicity and give the result of the calculation. In Sec. IV we describe the physical basis for the so-called "ledge" effect. Comments and conclusions are given in the last section. Throughout the paper we shall use the word multiplicity and the symbol n to refer to the charged-particle multiplicity.

II. GEOMETRICAL BRANCHING MODEL

We use the eikonal formalism to describe the cross sections

$$\sigma_{el}=\pi\int_0^\infty db^2(1-e^{-\Omega})^2 , \tag{2.1}$$

$$\sigma_{in}=\pi\int_0^\infty db^2(1-e^{-2\Omega}) , \tag{2.2}$$

$$\sigma_{tot}=2\pi\int_0^\infty db^2(1-e^{-\Omega}) , \tag{2.3}$$

in the approximation that the real part of the elastic scattering amplitude is zero. The eikonal function Ω here describes the opacity or absorption of the hadrons.

For $\sqrt{s}<100$ GeV were geometrical scaling is valid, one can approximate Ω by a function that depends on only one variable R:

$$\Omega_0(s,b)=\Omega_0(R) \tag{2.4}$$

where $b=b_0(s)R$. Thus all cross sections in (2.1)–(2.3) are proportional to $\sigma_0(s)$, where $\sigma_0(s)\equiv\pi b_0^2(s)$. A constant ratio $\sigma_{el}/\sigma_{tot}\approx 0.175$ can be obtained for a properly chosen $\Omega_0(R)$ (Refs. 15 and 16):

$$1-e^{-\Omega_0(R)}=0.712e^{-1.17R^2} . \tag{2.5}$$

Regarding Furry branching as the basic process of particle production in hadronic collisions at each impact parameter, it has been shown[6] that the multiplicity distribution

$$P_n^0=\int dR^2(1-e^{-2\Omega_0(R)})F_n^{k(R)} \tag{2.6}$$

possesses KNO scaling and that the calculated moments fit the experimental data well in the CERN ISR range, $\sqrt{s}\lesssim 65$ GeV. In Eq. (2.6), $F_n^{k(R)}$ is the Furry distribution

$$F_n^k(w)=\frac{\Gamma(n)}{\Gamma(k)\Gamma(n-k+1)}\left[\frac{1}{w}\right]^k\left[1-\frac{1}{w}\right]^{n-k} , \tag{2.7}$$

where

$$k(s,R)=\langle k\rangle(s)h(R) , \tag{2.8}$$

$$\bar{n}(s,R)=\langle n\rangle(s)h(R) , \tag{2.9}$$

$$h(R)=\frac{\Omega_0(R)}{(1-e^{-2\Omega_0(R)})\int dR^2\Omega_0(R)} \tag{2.10}$$

(Ref. 17), and $w=\langle n\rangle/\langle k\rangle=1+0.114\langle n\rangle$.

At higher energies it is assumed that geometrical scaling continues to be valid for soft interaction while jet production introduces a hard component and increases the absorption. The eikonal $\Omega(s,b)$ is then a sum of two components:

$$\Omega(s,b)=\Omega_0(s,b)+\Omega_1(s,b) . \tag{2.11}$$

$\Omega_0(s,b)$ is still defined by Eqs. (2.4) and (2.5), while $\Omega_1(s,b)$ is given by

$$\Omega_1(s,b)=\frac{\Omega_0(R)\sigma_{jet}}{2\sigma_0(s)\int dR^2\Omega_0(R)} . \tag{2.12}$$

σ_{jet} is the cross section for jet production

$$\sigma_{jet}=\int d(x_1x_2)\int_{-z_0}^{z_0}\frac{dz}{2}\frac{d\hat{\sigma}}{dz} , \tag{2.13}$$

where

$$z_0=[1-4(k_T^{min})^2/x_1x_2s]^{1/2} , \tag{2.14}$$

$$d(x_1x_2)=\frac{dx_1}{x_1}\frac{dx_2}{x_2}F(x_1)F(x_2) , \tag{2.15}$$

and

$$F(x)=G(x)+\tfrac{4}{9}[Q(x)+\bar{Q}(x)]=6.2e^{-9.5x} . \tag{2.16}$$

The last expression is the UA1 parametrization[18] for the gluon and quark distributions.[19] The hard-scattering differential cross section is

$$\frac{d\hat{\sigma}}{dz}=\frac{9\pi\alpha_s^2(Q^2)}{16x_1x_2s}\frac{(3+z^2)^3}{(1-z^2)^2} . \tag{2.17}$$

$k_T^{min}=2.7$ GeV is determined at one energy ($\sqrt{s}=540$ GeV) to fit total inelastic cross section while $\sigma_0(s)$ stays constant at 40 mb for $\sqrt{s}\geq 200$ GeV. The calculated σ_{el}/σ_{tot} is consistent with experimental data, which clearly show the violation of geometrical scaling.

Substituting Eq. (2.11) into (2.2), the inelastic cross section can be separated into soft and hard components in the conventional way:[20]

$$\sigma_{in}=\sigma^s+\sigma^h , \tag{2.18}$$

$$\sigma^s=\pi\int_0^\infty db^2(1-e^{-2\Omega_0})e^{-2\Omega_1} , \tag{2.19}$$

$$\sigma^h=\pi\int_0^\infty db^2(1-e^{-2\Omega_1}) . \tag{2.20}$$

σ^s is the soft component of the inelastic cross section without any hard scattering and σ^h is the component that has a hard scattering whether or not it is in conjunction with soft interaction. Accordingly, the multiplicity distribution can be written as

$$P_n=\frac{1}{\sigma_{in}}(\sigma^sP_n^s+\sigma^hP_n^h) , \tag{2.21}$$

$$\sigma^sP_n^s=\sigma_0(s)\int dR^2(1-e^{-2\Omega_0(R)})e^{-2\Omega_1(s,R)}F_n^{k(R)}(w) , \tag{2.22}$$

$$\sigma^h P_n^h=\sigma_0(s)\int dR^2(1-e^{-2\Omega_1(s,R)})H_n(s,R)\ . \quad (2.23)$$

$H_n(s,R)$ is the multiplicity distribution associated with jet production. With the notation

$$\mathcal{H}\{\cdots\}\equiv\frac{1}{\sigma_{\rm jet}}\int d(x_1x_2)\int_{-z_0}^{z_0}\frac{dz}{2}\frac{d\hat{\sigma}}{dz}(\cdots)\ , \quad (2.24)$$

we have

$$H_n(s,R)=\mathcal{H}\left[\sum_{ljm}\delta_{n,l+j+m}F_l^{k(R)}\Phi_j\Psi_m\right]\ , \quad (2.25)$$

where Φ_j is the multiplicity distribution of a jet fragmenting into j particles and Ψ_m is the distribution associated with the production of m particles by initial-state bremsstrahlung. In Ref. 15 it is assumed that

$$\Phi_j=\Psi_j=\frac{K^K}{\bar{j}\Gamma(K)}(j/\bar{j})^{K-1}e^{-Kj/\bar{j}}\ , \quad (2.26)$$

where $K=12$ is determined[21] by the phenomenology of the quark decay function in e^+e^- annihilation and $\bar{j}$ is the mean multiplicity of the produced particles, which depends on the virtuality $\hat{Q}^2$ according to

$$\bar{j}=0.35\ln\hat{Q}^2+0.38\ln^2\hat{Q}^2\ , \quad (2.27)$$

a parametrization adjusted to fit the high moments of the multiplicity distribution in $\bar{p}p$ collisions.[15]

III. MULTIPLICITY DEPENDENCE OF THE TRANSVERSE MOMENTUM

From the invariant inclusive momentum distribution $E\,d^3\sigma_n/d^3p$ for the production of n particles, the average transverse momentum $\langle p_T\rangle_n$ for n-particle production is

$$\langle p_T\rangle_n=\frac{1}{n\sigma_n}\int\frac{d^3p}{E}p_TE\frac{d^3\sigma_n}{d^3p}\ , \quad (3.1)$$

where $\sigma_n=\sigma_{\rm in}P_n$. In the GBM with jets, we have

$$E\frac{d^3\sigma_n}{d^3p}=\sigma_0\int_0^\infty dR^2(1-e^{-2\Omega_0})e^{-2\Omega_1}E\frac{d^3F_n^k}{d^3p}+\sigma_0\int_0^\infty dR^2(1-e^{-2\Omega_1})E\frac{d^3H_n}{d^3p}\ . \quad (3.2)$$

Because of (2.25), d^3H_n/d^3p in turn involves $d^3F_l^k/d^3p$, $d^3\Phi_j/d^3p$, and $d^3\Psi_m/d^3p$. We assume that these three functions are separately factorizable in their dependences on p and multiplicities, i.e.,

$$E\frac{d^3F_l^k}{d^3p}=lF_l^k(\bar{l})f(\mathbf{p},R)\ , \quad (3.3)$$

$$E\frac{d^3\Phi_j}{d^3p}=j\Phi_j(\bar{j})\phi(\mathbf{p},\hat{\mathbf{k}})\ , \quad (3.4)$$

$$E\frac{d^3\Psi_m}{d^3p}=m\Psi_m(\bar{m})\Psi(\mathbf{p},\hat{\mathbf{k}})\ , \quad (3.5)$$

where $\hat{\mathbf{k}}=(x_1x_2s)^{1/2}/2$ is the jet momentum. The momentum distributions satisfy the normalization

$$\int\frac{d^3p}{E}f(\mathbf{p},R)=\int\frac{d^3p}{E}\phi(\mathbf{p},\hat{\mathbf{k}})=\int\frac{d^3p}{E}\Psi(\mathbf{p},\hat{\mathbf{k}})=1\ , \quad (3.6)$$

$$\int\frac{d^3p}{E}\sum_l E\frac{d^3F_l^k}{d^3p}=\sum_l lF_l^k=\bar{l}\ , \quad (3.7)$$

and similarly for Φ_j and Ψ_m, giving rise to $\bar{j}$ and $\bar{m}$, respectively. Using (3.3)–(3.5) and (2.25) we obtain

$$E\frac{d^3H_n}{d^3p}=\mathcal{H}\left[\sum_{ljm}\delta_{n,l+j+m}F_l^k\Phi_j\Psi_m(lf+j\phi+m\Psi)\right]\ . \quad (3.8)$$

To proceed, we need to specify f, ϕ, and Ψ, none of which are known very well from first principles. We have assumed (here and in Ref. 14) that the properties of soft production in the presence of jets are unchanged from those in the absence of jets. For the momentum distribution $f(\mathbf{p},R)$ the factorizable form in (3.3) is an approximation that ignores energy conservation for an l-body system. Taking that constraint into account by means of the Darwin-Fowler method would result in a distribution characterized by a partition temperature,[22] which has the effect of damping $dN/d\eta$ at large pseudorapidity η for high-multiplicity events. In Ref. 22 the transverse cutoff is put in additionally by hand. In our more simple treatment of $f(\mathbf{p},R)$ we adopt the canonical p_T distribution with no dependence on rapidity:

$$f(\mathbf{p},R)=[\pi Y\bar{p}_T^2(R)]^{-1}\exp[-2p_T/\bar{p}_T(R)]\ , \quad (3.9)$$

where $Y=\ln(\sqrt{s}/\bar{p}_T)$; it is normalized to satisfy (3.6). The average p_T calculated from (3.9) is $\bar{p}_T$. We allow an R dependence in $\bar{p}_T(R)$ for reasons to be explained below.

For the hadron distribution in a jet we assume that the longitudinal-momentum distribution along the jet axis is given by the fragmentation function $D(x,\hat{\mathbf{k}})$ measured in e^+e^- annihilation, and that there is no significant spreading in the cone around the jet axis. Thus, we have

$$\phi(\mathbf{p},\hat{\mathbf{k}})=(\pi\bar{j})^{-1}\int dx\,\delta(y_p-y_k)\delta(p_T^2-x^2k_T^2)D(x,\hat{\mathbf{k}})\ , \quad (3.10)$$

where $D(x,\hat{\mathbf{k}})$ is the noninvariant parton decay function normalized by

$$\int_0^1 D(x,\hat{\mathbf{k}})dx=\bar{j}(\hat{\mathbf{k}})\ , \quad (3.11a)$$

$$\int_0^1 D(x,\hat{\mathbf{k}})x\,dx=\tfrac{2}{3}\ , \quad (3.11b)$$

$\bar{j}(\hat{\mathbf{k}})$ being the average number of (charged) particles in a jet of momentum $\hat{\mathbf{k}}$, and the $\frac{2}{3}$ factor being the average fraction of charged particles in a jet.

The momentum distribution $\Psi(\mathbf{p},\hat{\mathbf{k}})$ due to bremsstrahlung in the initial state before the hard vertex is the most difficult one to ascertain. We have virtually no theoretical or empirical guidance on its nature, except that as a possible mechanism for the pedestal effect[10,11] it contributes to the background of a peak (due to a jet) in $dE_T/d\eta$ vs η in such a substantial way that it nearly dou-

bles the minimum-bias background. Since the enhancement of the background increases with both the E_T of the jet and the c.m. energy of the hadronic collision, we parametrize the average transverse momentum in $\Psi(\mathbf{p},\hat{\mathbf{k}})$ by

$$\langle p_T\rangle_\Psi = A_0(x_1x_2)^\alpha s^\beta . \tag{3.12}$$

A determination of the parameters A_0, α, and β will be described below. Combining (3.1)–(3.3) with (3.8), we obtain, for the production of n massless pions,

$$\langle p_T\rangle_n = \frac{\sigma_0}{\sigma_n}\left\{\int dR^2(1-e^{-2\Omega_0})e^{-2\Omega_1}F_n^{k(R)}\bar{p}_T(R) + \int dR^2(1-e^{-2\Omega_1})\mathcal{H}\left[\sum_{ljm}\delta_{n,l+j+m}F_l^{k(R)}\Phi_j\Psi_m\frac{1}{n}\left[l\bar{p}_T(R)+\frac{2j}{3\bar{j}}[x_1x_2s(1-z^2)]^{1/2}+m\langle p_T\rangle_\Psi\right]\right]\right\} . \tag{3.13}$$

The overall average transverse momentum is

$$\langle p_T\rangle = \sum_{n=0}^{\infty}\langle p_T\rangle_n P_n = \frac{1}{\sigma_{\rm in}}\sum_{n=0}^{\infty}\langle p_T\rangle_n\sigma_n . \tag{3.14}$$

To determine the parameters A_0, α, and β, we first define the quantity

$$\langle\tilde{p}_T\rangle = \langle n\rangle^{-1}\sum_{n=0}^{\infty} n\langle p_T\rangle_n P_n . \tag{3.15}$$

Using (3.13) the summation over n can be carried out to yield

$$\langle\tilde{p}_T\rangle = \frac{\sigma_0}{\langle n\rangle\sigma_{\rm in}}\left[\int dR^2(1-e^{-2\Omega_0})e^{-2\Omega_1}\bar{n}(s,R)\bar{p}_T(R)+\int dR^2(1-e^{2\Omega_1})\mathcal{H}\left\{\bar{l}\bar{p}_T(R)+\tfrac{2}{3}[x_1x_2s(1-z^2)]^{1/2}+\bar{m}\langle p_T\rangle_\Psi\right\}\right] . \tag{3.16}$$

Note that (3.16) does not explicitly depend on the distributions F_l^k, Φ_j, or Ψ_m. From the experimental data[8,10–12,23] on $\langle p_T\rangle_n$ and P_n, we can determine the empirical values of $\langle\tilde{p}_T\rangle$ at four energies by using (3.15).

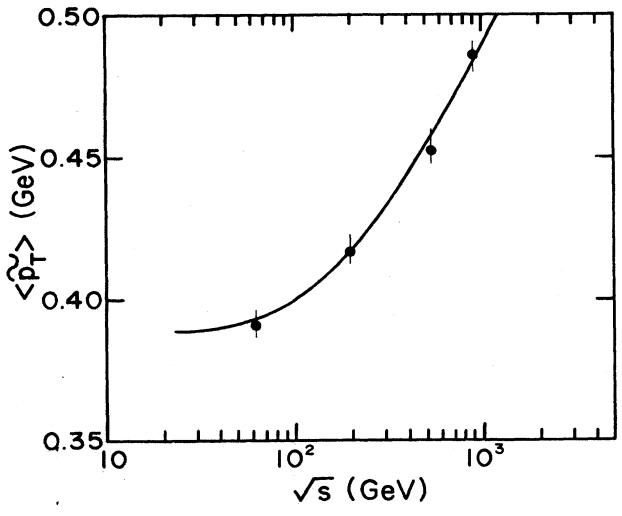

FIG. 1. $\langle\tilde{p}_T\rangle$ is a quantity defined by (3.15). The experimental values of this quantity are determined by using the data for $\langle p_T\rangle_n$ from Refs. 10–12 and 23 and for P_n from Ref. 8. The theoretical curve is calculated as described in the text.

In performing that computation it is necessary to assume large-n behaviors of $\langle p_T\rangle_n$ and P_n beyond the measured values of n. We have adopted the assumption that $\langle p_T\rangle_n$ saturates at large n and that P_n satisfies the empirical form of negative-binomial distribution.[8] The result is shown as four experimental points in Fig. 1. It should be mentioned that the data on $\langle p_T\rangle_n$ and P_n are obtained from different experiments: $\langle p_T\rangle_n$ form UA1 (Refs. 10, 11, and 23) and Ames-Bologna-CERN-Dormund-Heidelberg-Warsaw (ABCDHW) (Ref. 12), and P_n from UA5 (Ref. 8). The experiments on $\langle p_T\rangle_n$ all have a cut on pseudorapidity: $\eta_{\rm cut}=2.5$, but the data we have used for P_n are for the full η range (even though UA5 has data for various $\eta_{\rm cut}$). The reason for this disparity is that the geometrical branching model has not yet been developed to the point of describing the η dependence, when jets are present. Thus we use P_n for the full η range, for which the theoretical description is ready at hand, and calculate the artificial hybrid quantity $\langle\tilde{p}_T\rangle$ in (3.15), which in itself has no phenomenological significance, but is a convenient intermediate step for us to determine the unknown parameters, as we now explain.

To calculate $\langle\tilde{p}_T\rangle$ in the GBM with jets we use (3.16). The parameter $\bar{p}_T(R)$ controls the average p_T of the soft processes and is mainly responsible in fitting $\langle\tilde{p}_T\rangle$ at $\sqrt{s}=63$ GeV. At higher energies the contributions from jets and bremsstrahlung become important, and the parameters in (3.12) are to be adjusted to fit the other data

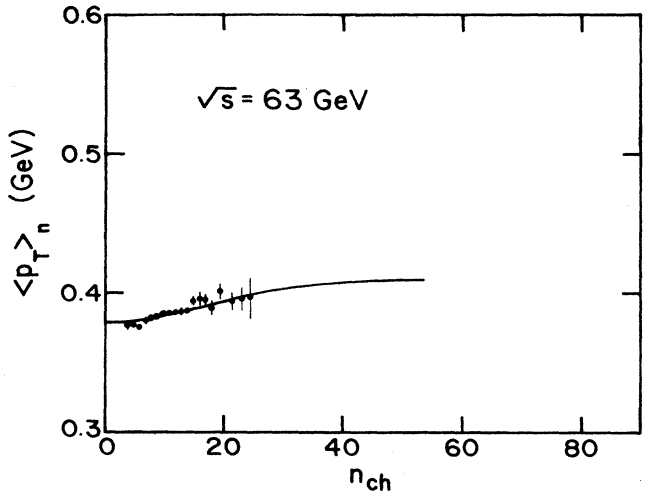

FIG. 2. The data are from ABCDHW (Ref. 12); the curve is the calculated result.

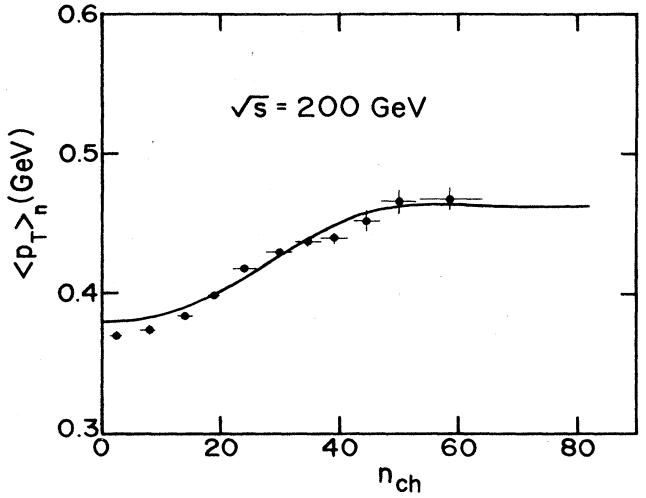

FIG. 3. The data are from UA1 (Refs. 10, 11, and 23); the curve is the calculated theoretical result.

points in Fig. 1. In determining $\bar{p}_T$ we take note of the fact that even at $\sqrt{s}=63$ GeV, the measured values of $\langle p_T \rangle_n$ depend on the multiplicity n (Ref. 12). Since jet contribution is insignificant in the ISR energy range, the only way that we can achieve such a dependence in our model is to introduce an R dependence in $\bar{p}_T(R)$, since the average multiplicity depends on R. We have found that

$$\bar{p}_T(R)=0.38+0.015e^{-0.8R^2}\ (\mathrm{GeV}/c) \tag{3.17}$$

can adequately reproduce the $\langle p_T \rangle_n$ vs n dependence shown in Fig. 2. With this parametrization fixed in (3.13), we then go to higher energies and vary A_0, α, and β in (3.12) to fit the data in Fig. 1. The result is shown by the curve in Fig. 1 for the values

$$A_0=0.19,\quad \alpha=0.06,\quad \beta=0.30\ . \tag{3.18}$$

It should be emphasized that the construction of $\langle \tilde{p}_T \rangle$ and the subsequent fit of that quantity are only intermediate steps of our problem of the determination of $\langle p_T \rangle_n$. Because (3.16) does not involve the multiplicity distribution functions, it does not have the full content of (3.13). We have used the experimental values for the s dependence of $\langle \tilde{p}_T \rangle$ to determine the unknown parameters in (3.12). Once they are fixed, we can calculate the n dependence of $\langle p_T \rangle_n$ at various energies without any more freedom. It is there where predictions are made in this model.

Before showing the results, we remark that our aim in this paper is not to elucidate the pedestal problem.[10,11,23] We have not considered the rapidity dependence of the produced particles. We have varied the parameters in (3.12) to fit the s dependence of $\langle \tilde{p}_T \rangle$, but the values determined shed no direct light on $dE_T/d\eta$, in terms of which the pedestal problem is made manifest. Instead, the parametrized form for $\langle p_T \rangle_\psi$ enables us to calculate $\langle p_T \rangle_n$. Put differently, although both $dE_T/d\eta$ and $\langle p_T \rangle_n$ can be affected by initial-state bremsstrahlung, there is no direct relationship between the two, at least not until there is an independent determination of $dE_T/d\eta$; thus a better understanding of one does not necessitate a clarification of the other. Indeed, the pedestal problem is one worthy of a separate investigation in its own right.

The results of our calculation for $\langle p_T \rangle_n$ are shown in Figs. 3–6. They should be valid only for $|\eta|<2.5$. That is because of the way in which the data in Fig. 1 are determined, as we have explained above. The curves in Figs. 3–5, which are the calculated results, agree very well with the data from UA1 (Refs. 10, 11, and 23), which are for $|\eta|<2.5$. Note that at each energy between 200 and 900 GeV there is a rise in $\langle p_T \rangle_n$ with n—the higher the energy, the steeper the rise. The rise is followed by a plateau, commencing at around $n=50$ in each case.

What is not originally anticipated, but turns out to be very exciting, is that when the calculation is pushed to higher values of n beyond the measured multiplicities, we find $\langle p_T \rangle_n$ to increase again. This rise-plateau-rise (ledge) phenomenon is an intrinsic feature of our two-component model, independent of the details of parametrization, as we shall explain in the next section. Very recently, data obtained at the C0 intersection region of the Fermilab $\bar{p}p$ collider at $\sqrt{s}=1.8$ TeV have become available[24] and they indeed confirm the existence of the second rise, as shown in Fig. 6. We regard this as a strong support for the GBM with jets.

IV. THE LEDGE EFFECT

The results of our calculation discussed in the preceding section reveals the rise-plateau-rise structure of $\langle p_T \rangle_n$ vs n, which we refer to hereafter as the ledge effect, for brevity. In this section we describe the physical mechanism for the phenomenon, and contrast it with a similar behavior conjectured earlier as a signature for phase transition[3] in ultrarelativistic nuclear collisions.

To see how the first rise is developed as shown in Figs. 3–5, we begin by noting that the mechanism is different from the gentle rise seen in Fig. 2. At $\sqrt{s}=63$ GeV, our model still describes geometrical scaling with $\Omega_1(s,R)$

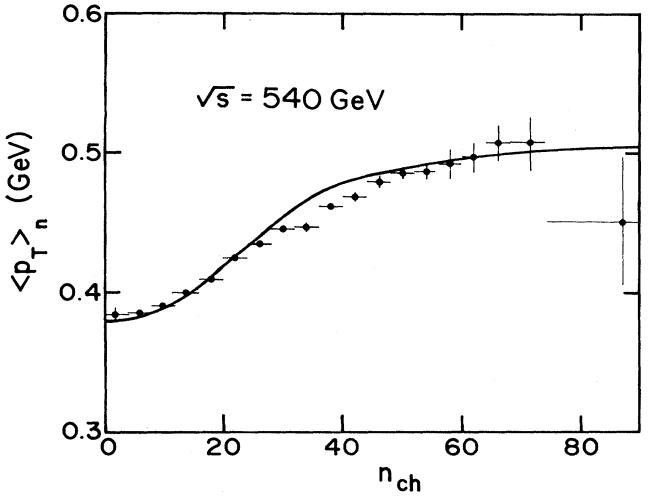

FIG. 4. The data are from UA1 (Refs. 10 and 23); the curve is the calculated theoretical results.

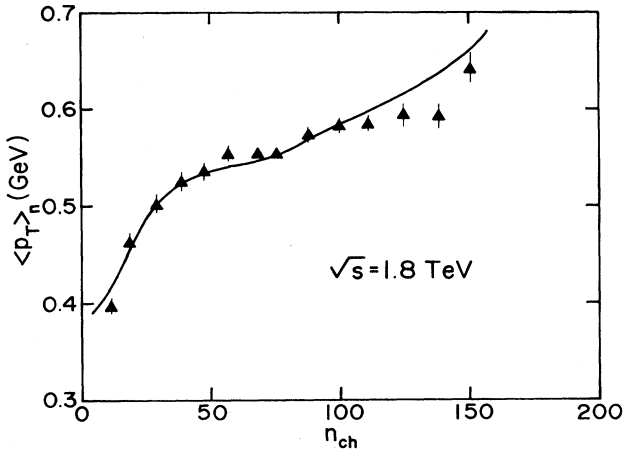

FIG. 6. The data are from C0 (Ref. 24); the curve is the calculated theoretical result.

$=0$. The increase of $\langle p_T \rangle_n$ in Fig. 2 is achieved through an R dependence in $\bar{p}_T$ as given in (3.17). This is a fitted result, as we do not pretend to have any prediction on the average p_T of soft processes, let alone its R dependence. The increase of $\bar{p}_T$ with decreasing R seems reasonable, since a central collision is more violent and is expected to have larger $\bar{p}_T$ (especially if one thinks in the context of a thermodynamical picture).

On the other hand, the mechanism responsible for the rise in Figs. 3–5 is intimately related to the jet production in our model. Qualitatively, one expects jets to contribute to high-p_T particles, so it seems that any model with jets would give rise to the increase in $\langle p_T \rangle$. However, to understand the ledge effect, it is necessary to examine the mechanism more closely. Let us focus on (3.13). The first line in that equation describes the contribution from events with soft production only without any hard interaction; $\bar{p}_T(R)$ is the average p_T for collisions at R. The second line of that equation describes the average p_T contribution arising from three sources in an event with jet: soft interaction, jet fragmentation, and initial-state bremsstrahlung. Because of the latter two additional sources, we know that the average p_T of events with jets would be higher than $\bar{p}_T(R)$. For the moment let us not scrutinize the details of those two terms, but just regard the term $(1/n)(\cdots)$ as a quantity greater than $\bar{p}_T(R)$. Our question now is the following: at fixed s, as n is increased, how does $\langle p_T \rangle_n$ change? Apart from the normalization factor σ_n^{-1} the first line depends on n through $F_n^{k(R)}$ only. Since R is a variable to be integrated, as n increases, $F_n^{k(R)}$ receives greater contribution from larger $k(R)$, which in turn puts greater emphasis on the small-R part of the integration. The same can be said about the second integral in (3.13). Thus the relative importance between the first and second integrals is controlled by the two weighting factors: $(1-e^{-2\Omega_0(R)})e^{-2\Omega_1(R)}$ vs $1-e^{-2\Omega_1(R)}$. From (2.5) and (2.12) one finds that when $\sigma_{\text{jet}}/\sigma_0$ is not negligible, the former factor decreases with decreasing R, while the latter increases. Thus the changes in the weighting factors favor the hard contribution, as n increases at fixed s. Since, the second line of (3.13) contributes an average p_T larger than $\bar{p}_T(R)$, $\langle p_T \rangle_n$ increases with n as shown in Figs. 3–5. The above mechanism has little to do with the details of the jet fragmentation process. In fact, it relies so much on the manner in which the eikonal functions appear in the weighting factors that it is instructive to mention an alternative calculation. Suppose that one separates the soft and hard components according to the weighting factors $1-e^{-2\Omega_0}$ and $(1-e^{-2\Omega_1})e^{-2\Omega_0}$, respectively. One would find that the resultant n dependence of $\langle p_T \rangle_n$ will look distinctly different from the data. The proper factors are, however, the ones shown in (2.22) and (2.23) for reasons explained in Ref. 14. In this respect, our model differs significantly from other two-component models, in which the eikonal functions do not play a central role, such as in Refs. 18, 25, and 26.

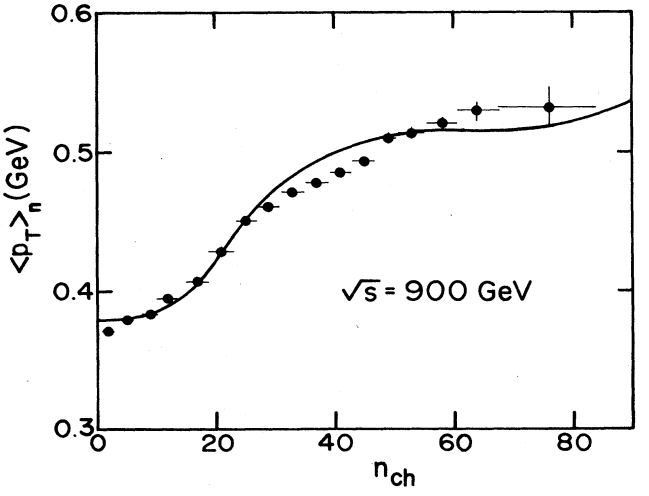

FIG. 5. The data are from UA1 (Refs. 10, 11, and 23); the curve is the calculated theoretical result.

The second rise in the ledge phenomenon is associated with the properties of jet fragmentation. The increase of n may originate in the increase of j. The fragmentation

function Φ_j, as given in (2.26), is damped rapidly at high j for a fixed $\bar{j}$. But since the average multiplicity $\bar{j}$ increases with virtually [as indicated in (2.27)], the subset of high-j events favors high virtuality, which is not forbidden because the integrations over x_1, x_2, and z in $\mathcal{H}\{\cdots\}$ allow hard jets at high s. Now, in the second line of (3.13) the middle term is $4j\hat{\mathbf{k}}\sin\theta/3\bar{j}$, in which $\hat{\mathbf{k}}\sin\theta$ is the average transverse momentum of the whole jet, so $\hat{\mathbf{k}}\sin\theta/\bar{j}$ is the average transverse momentum per particle in the jet. At high virtuality, $\bar{j}$ is large, but $\hat{\mathbf{k}}$ is larger, so the ratio increases with virtuality. For this chain of reasons, when n is very large, the large-j part contributes with high average p_T, resulting in further increases in $\langle p_T\rangle_n$.

Note that the first rise is associated with the smearing in R^2, while the second is associated with the integrations over the parton momenta and over their scattering angle. The former is a consequence of an adjustment of the dominance from soft to hard contribution, while the latter is a kind of trigger bias, i.e., the selection of high-n events favors the type of events with high-momentum jets and therefore high p_T [similar to the trigger bias associated with high-p_T jets measured at CERN ISR (Ref. 27)]. Such a trigger bias usually occurs at the kinematical boundary. In our case here it is for very high n at a fixed s. The mismatch between the multiplicities at which the two rises occur results in the ledge effect.

V. CONCLUSION

We have shown that the geometrical branching model with jets is a formalism capable of describing the multiplicity dependence of the average transverse momentum. There are many inputs in the model, most of which are fixed by other previous considerations, but some are new. We have in this paper adjusted the parametrization of initial-state bremsstrahlung in order to obtain the correct s dependence of $\langle p_T\rangle$. Our results on $\langle p_T\rangle_n$ then agree well with data.

Independent of the details of the above-mentioned parametrization, the significance of our finding in this work is that the (rise-plateau-rise) ledge effect is a necessary consequence of our model. The first rise is due to the dominance of the hard processes over the soft component; the second rise is due to the nature of jet production and fragmentation. Up to 900 GeV only the first rise is prominent. The recent data at 1.8 TeV give encouraging support for the second rise.

The ledge effect described here for $\bar{p}p$ collisions may be related to the similar structure seen in nuclear collisions in the cosmic-ray data. We are not certain. As discussed in the Introduction, hydrodynamical expansion alone cannot account for the second rise. We have conjectured the possible influence of jet production. Now that we have demonstrated the existence of this ledge effect in hadronic collisions, it provides the needed encouragement to investigate the more difficult problem of jet production in quark-gluon plasma. If it can account for the second rise in nuclear collisions, as observed experimentally, then the ledge effect cannot be used naively as a signal for the formation of quark matter. Jet production rather than high-temperature plasma would be cause of high $\langle p_T\rangle_n$. Nevertheless, the structure of the n dependence of $\langle p_T\rangle_n$ may be influenced by the presence of plasma so that perhaps in a subtle way one may still see some signature of phase transition. At this pont we have no basis for any more definitive speculation.

Our work in this paper therefore has achieved two objectives. On the one hand, we have added one more topic to the list of testing grounds where the geometrical branching model with jets has successfully confronted the data. They include KNO scaling and violation, geometrical scaling and violation, forward-backward multiplicity correlation, rapidity interval dependence, and now multipicity dependence of average transverse momentum. On the other hand, it predicts the ledge effect, which is confirmed by the Tevatron collider data. Consequently, it provides the welcome stimulus needed to investigate whether jet production is also responsible for the similar ledge effect seen in the JACEE data.

ACKNOWLEDGMENTS

We thank Wei R. Chen for many helpful discussions. This work was supported in part by the U.S. Department of Energy under Grant No. DE-FG06-85ER40224.

[1]X. N. Wang and R. C. Hwa, Phys. Rev. D **35**, 3409 (1987).
[2]T. H. Burnett *et al.*, Phys. Rev. Lett. **50**, 2062 (1983).
[3]L. Van Hove, Phys. Lett. **118B**, 138 (1982).
[4]R. C Hwa, in *Hadrons, Quarks, and Gluons,* proceedings of 22nd Rencontre de Moriond, Les Arcs, France, 1987, edited by J. Tran Thanh Van (Editions Frontiéres, Gif-sur-Yvette, 1987), p. 483.
[5]Z. Koba, H. N. Nielsen, and P. Olesen, Nucl. Phys. **B40**, 317 (1972).
[6]W. R. Chen and R. C. Hwa, Phys. Rev. D **36**, 760 (1987).
[7]W. H. Furry, Phys. Rev. **52**, 569 (1937); N. Arley, *Stochastic Processes and Cosmic Radiation* (Wiley, New York, 1948), p. 92.
[8]G. J. Alner *et al.*, Phys. Lett. **160B**, 193 (1985); **107B**; 476 (1986).
[9]G. Arneson *et al.*, Phys. Lett. **118B**, 167 (1982).
[10]G. Piano-Mortari, in *Proceedings of the Oregon Meeting,* Annual Meeting of the Division of Particles and Fields of the APS, Eugene, Oregon, 1985, edited by R. C. Hwa (World Scientific, Singapore, 1986), p. 615.
[11]A. Norton, in *Multiparticle Production,* proceedings of the Shandong Workshop, Jinan, China, 1987, edited by R. C. Hwa and Q. B. Xie (World Scientific, Singapore, 1988), p. 87.
[12]A. Breakstone *et al.*, Phys. Lett. **132B**, 463 (1983).
[13]G. Pancheri and Y. Srivastava, Phys. Lett. **159B**, 69 (1985).
[14]R. C. Hwa, Phys. Rev. D **37**, 1830 (1988).
[15]W. R. Chen and R. C. Hwa, preceding paper, Phys. Rev. D **39**, 179 (1989).
[16]A. W. Chao and C. N. Yang, Phys. Rev. D **8**, 2063 (1973).
[17]W. R. Chen, R. C. Hwa, and X. N. Wang, Phys. Rev. D **38**,

3394 (1988).
[18]G. Pancheri and Y. N. Srivastava, Phys. Lett. B **182**, 199 (1986).
[19]F. Halzen and P. Hoyer, Phys. Lett. **130B**, 326 (1983).
[20]L. Durand and H. Pi, Phys. Rev. Lett. **58**, 303 (1987).
[21]M. Derrick *et al.*, Phys. Lett. **168B**, 299 (1986).
[22]T. T. Chou, C. N. Yang, and E. Yen, Phys. Rev. Lett. **54**, 510 (1985).
[23]G. Ciapetti, in *Proton-Antiproton Collider Physics,* proceedings of the Fifth Topical Workshop, St. Vincent, Italy, 1985, edited by M. Greco (World Scientific, Singapore, 1985), p. 488.
[24]T. Alexopoulos *et al.,* Phys. Rev. Lett. **60**, 1622 (1988).
[25]T. K. Gaisser, F. Halzen, A. D. Martin, and C. J. Maxwell, Phys. Lett. **166B**, 219 (1986).
[26]T. Sjorstrand and M. van Zijl, Phys. Rev. D **36**, 2019 (1987).
[27]S. Ellis, M. Jacob, and P. Landshoff, Nucl. Phys. **B108**, 93 (1976).